Korean J. Chem. Eng., **25**(1), 34-40 (2008)

Transient free convection flow over an isothemal vertical cylinder with temperature dependent viscosity

Hari Ponnamma Rani and Chang Nyung Kim†

Department of Mechanical Engineering, College of Advanced Technology (Industrial Liaison Research Institute), Kyung Hee University, Gyeonggi-do 446-701, Korea
(*Received 23 March 2007 • accepted 2 August 2007*)

Abstract−A numerical analysis is performed to study the influence of temperature-dependent viscosity and Prandtl number on unsteady laminar free convection flow over a vertical cylinder. The governing boundary layer equations are converted into a non-dimensional form and a Crank-Nicolson type of implicit finite-difference method is used to solve the governing non-linear set of equations. Numerical results are obtained and presented for different viscosity-variation parameters and Prandtl numbers. Transient effects of velocity and temperature are analyzed. The heat transfer characteristics against the viscosity-variation parameter are analyzed with the help of average skin-friction and Nusselt number and are shown graphically.

Key words: Transient, Natural Convection, Vertical Cylinder, Variable Viscosity, Finite Difference Method

INTRODUCTION

Unsteady natural convection flow of a viscous incompressible fluid over a heated vertical cylinder is an important problem relevant to many engineering applications. The exact solution for these types of non-linear problems is still out of reach. Sparrow and Gregg [1] provided the first approximate solution for the laminar buoyant flow of air bathing a vertical cylinder heated with a prescribed surface temperature, by applying the similarity method and power series expansion. Minkowycz and Sparrow [2] obtained the solution for the same problem using the non-similarity method. Fujii and Uehara [3] analyzed the local heat transfer results for arbitrary Prandtl numbers. Lee et al. [4] investigated the problem of natural convection in laminar boundary layer flow along slender vertical cylinders and needles for the power-law variation in wall temperature. Dring and Gebhart [5] presented the transient natural convection results in association with the thin wires in liquids. Velusamy and Garg [6] presented the numerical solution for transient natural convection over heat-generating vertical cylinders of various thermal capacities and radii. The rate of propagation of the leading edge effect was given special consideration by them. Recently, Rani [7] has investigated the unsteady natural convection flow over a vertical cylinder with variable heat and mass transfer using the finite difference method.

All the above studies were confined to a fluid with constant viscosity. However, it is known that this physical property may change significantly with temperature [8]. Also, the viscosity of a fluid is a measure of its resistance to the flow and changes with respect to the temperature. Hence, to predict accurately the flow behavior, it is necessary to consider the variation of viscosity in the flow problems. Gray et al. [9] showed that when the effect of change in viscosity is considered, the flow characteristics may be substantially changed compared to the case with constant viscosity. Kafoussius and Rees [10] investigated the effect of temperature dependent viscosity on mixed convection flow over a vertical flat plate. Recently, Hossain et al. [11] investigated the natural convection flow over a vertical wavy cone with variable viscosity, which depends linearly on the temperature. From the above investigations it is found that the variation of viscosity with temperature is an interesting macroscopic physical phenomenon in fluid mechanics.

The unsteady natural convection flow of a viscous incompressible fluid over a heated vertical cylinder with variation of viscosity has received very scant attention in the literature. Hence in the present investigation our attention is focused on the boundary-layer regime caused by a uniformly heated vertical cylinder that is immersed in a fluid with temperature dependent viscosity. The surface temperature of the cylinder is considered higher than that of the ambient fluid temperature. A semi-empirical formula for the viscosity versus temperature proposed by Ling and Dybbs [12] is employed in the present study. The governing non-dimensional unsteady partial differential equations are solved numerically by using the implicit finite-difference scheme. The effect of the viscosity variation on the velocity and temperature with respect to time, and on the average Nusselt number and the skin-friction is shown.

Let us begin in section 2 with a detailed description about the formulation of the problem. The conservation laws for mass, momentum and energy equations of the incompressible fluid flow past a semi-infinite vertical cylinder are detailed. In section 3 the details about the grid generation and numerical methods for solving the Navier-Stokes and energy equations are given. In section 4 the two-dimensional transient velocity and temperature profiles are analyzed for various values of viscosity-variation parameters and Prandtl numbers. The average skin-friction and heat transfer rates are also elucidated. Finally, of course, the concluding remarks are made.

FORMULATION OF THE PROBLEM

An unsteady two-dimensional laminar natural convection boundary layer flow of a viscous incompressible fluid past a uniformly heated semi-infinite vertical cylinder of radius r_0 is considered as

†To whom correspondence should be addressed.
E-mail: cnkim@khu.ac.kr

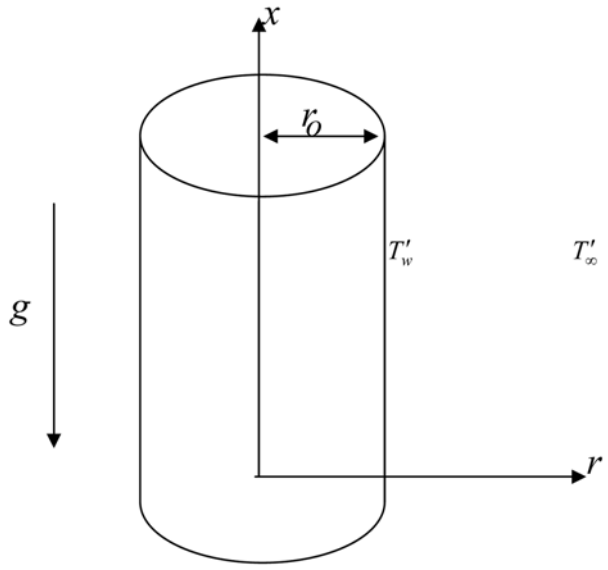

Fig. 1. Schematic of the investigated problem.

shown in Fig. 1. The x-axis is measured vertically upward along the axis of the cylinder. The origin of x is taken to be at the leading edge of the cylinder, where the boundary layer thickness is zero. The radial coordinate r is measured perpendicular to the axis of the cylinder. The surrounding stationary fluid temperature is assumed to be of ambient temperature (T'_∞). Initially, i.e., at time $t'=0$ it is assumed that the cylinder and the fluid are of the same temperature T'_∞. When $t'>0$, the temperature of the cylinder is raised to T'_w ($>T'_\infty$) and maintained at the same level for all time $t'>0$. It is assumed that the effect of viscous dissipation is negligible in the energy equation. Under these assumptions, the boundary layer equations of mass, momentum and energy with Boussinesq's approximation are as follows:

$$\frac{\partial(ru)}{\partial x}+\frac{\partial(rv)}{\partial r}=0 \tag{1}$$

$$\frac{\partial u}{\partial t'}+u\frac{\partial u}{\partial x}+v\frac{\partial u}{\partial r}=g\beta(T'-T'_\infty)+\frac{1}{\rho r}\frac{\partial}{\partial r}\left(\mu r\frac{\partial u}{\partial r}\right) \tag{2}$$

$$\frac{\partial T'}{\partial t'}+u\frac{\partial T'}{\partial x}+v\frac{\partial T'}{\partial r}=\frac{\alpha}{r}\frac{\partial}{\partial r}\left(r\frac{\partial T'}{\partial r}\right) \tag{3}$$

where u and v are the velocity components parallel to x and r coordinates, respectively, g is the acceleration due to the gravity, β is the volumetric coefficient of thermal expansion, ρ is the density, α is the thermal diffusivity and $\mu(T')$ is the viscosity of the fluid depending on the temperature T' of the fluid.

Out of the many forms of viscosity variation available in the literature we have considered the following form introduced by Ling and Dybbs [12] and also used by Molla et al. [13]:

$$\mu(T')=\frac{\mu_\infty}{1+b(T'-T'_\infty)} \tag{4}$$

where b is a constant and μ_∞ is the viscosity of the ambient fluid.

The initial and boundary conditions are given by

$$\begin{aligned} &t'\le 0: u=0, v=0, T'=T'_\infty && \text{for all x and r}\\ &t'>0: u=0, v=0, T'=T'_w && \text{at } r=r_0\\ &\quad u=0, v=0, T'=T'_\infty && \text{at } x=0\\ &\quad u\to 0, v\to 0, T'\to T'_\infty, && \text{as } r\to\infty \end{aligned} \tag{5}$$

Now, the following non-dimensional quantities are introduced:

$$X=Gr^{-1}\frac{x}{r_0},\ R=\frac{r}{r_0},\ U=Gr^{-1}\frac{ur_0}{\upsilon},\ V=\frac{vr_0}{\upsilon},\ t=\frac{\upsilon t'}{r_0^2},\ T=\frac{T'-T'_\infty}{T'_w-T'_\infty},$$
$$\lambda=b(T'_w-T'_\infty)\ \ Gr=\frac{g\beta r_0^3(T'_w-T'_\infty)}{\upsilon^2},\ \ Pr=\frac{\upsilon}{\alpha} \tag{6}$$

where $\upsilon(=\mu_\infty/\rho)$ is the reference kinematic viscosity, λ, Gr and Pr denote the viscosity-variation parameter, the Grashof number and the Prandtl number, respectively.

By introducing the above non-dimensional quantities into the Eqs. (1)-(3), they are reduced to the following form.

$$\frac{\partial U}{\partial X}+\frac{\partial V}{\partial R}+\frac{V}{R}=0 \tag{7}$$

$$\frac{\partial U}{\partial t}+U\frac{\partial U}{\partial X}+V\frac{\partial U}{\partial R}=T+\frac{1}{(1+\lambda T)}\left(\frac{\partial^2 U}{\partial R^2}+\frac{1}{R}\frac{\partial U}{\partial R}\right)-\frac{\lambda}{(1+\lambda T)^2}\frac{\partial T}{\partial R}\frac{\partial U}{\partial R} \tag{8}$$

$$\frac{\partial T}{\partial t}+U\frac{\partial T}{\partial X}+V\frac{\partial T}{\partial R}=\frac{1}{Pr}\left(\frac{\partial^2 T}{\partial R^2}+\frac{1}{R}\frac{\partial T}{\partial R}\right) \tag{9}$$

The corresponding initial and boundary conditions in non-dimensional quantities are given by

$$\begin{aligned} &t\le 0: U=0, V=0, T=0 && \text{for all X and R}\\ &t>0: U=0, V=0, T=1 && \text{at } R=1\\ &\quad U=0, V=0, T=0 && \text{at } X=0\\ &\quad U\to 0, V\to 0, T\to 0 && \text{as } R\to\infty \end{aligned} \tag{10}$$

NUMERICAL SOLUTION OF THE PROBLEM

In order to solve the unsteady coupled non-linear governing Eqs. (7)-(9) an implicit finite difference scheme of Crank-Nicolson type has been employed. The finite difference equations corresponding to Eqs. (7)- (9) are as follows:

$$\frac{U_{i,j}^{k+1}-U_{i-1,j}^{k+1}+U_{i,j}^{k}-U_{i-1,j}^{k}}{2\Delta X}+\frac{V_{i,j}^{k+1}-V_{i,j-1}^{k+1}+V_{i,j}^{k}-V_{i,j-1}^{k}}{2\Delta R}+\frac{V_{i,j}^{k+1}}{1+(j-1)\Delta R}=0 \tag{11}$$

$$\begin{aligned}&\frac{U_{i,j}^{k+1}-U_{i,j}^{k}}{\Delta t}+\frac{U_{i,j}^{k}}{2\Delta X}(U_{i,j}^{k+1}-U_{i-1,j}^{k+1}+U_{i,j}^{k}-U_{i-1,j}^{k})\\ &\quad+\frac{V_{i,j}^{k}}{4\Delta R}(U_{i,j+1}^{k+1}-U_{i,j-1}^{k+1}+U_{i,j+1}^{k}-U_{i,j-1}^{k})=\frac{T_{i,j}^{k+1}+T_{i,j}^{k}}{2}\\ &\quad+A\left\{\frac{U_{i,j-1}^{k+1}-2U_{i,j}^{k+1}+U_{i,j+1}^{k+1}+U_{i,j-1}^{k}-2U_{i,j}^{k}+U_{i,j+1}^{k}}{2(\Delta R)^2}\right.\\ &\quad\left.+\frac{U_{i,j+1}^{k+1}-U_{i,j-1}^{k+1}+U_{i,j+1}^{k}-U_{i,j-1}^{k}}{4[1+(j-1)\Delta R]\Delta R}\right\}\\ &\quad-\lambda A^2\frac{U_{i,j+1}^{k+1}-U_{i,j-1}^{k+1}+U_{i,j+1}^{k}-U_{i,j-1}^{k}}{4\Delta R}\frac{T_{i,j+1}^{k+1}-T_{i,j-1}^{k+1}+T_{i,j+1}^{k}-T_{i,j-1}^{k}}{4\Delta R}\end{aligned} \tag{12}$$

$$\frac{T_{i,j}^{k+1}-T_{i,j}^{k}}{\Delta t}+\frac{U_{i,j}^{k}}{2\Delta X}(T_{i,j}^{k+1}-T_{i-1,j}^{k+1}+T_{i,j}^{k}-T_{i-1,j}^{k})$$

$$+\frac{V^{k}_{i,j}}{4\Delta R}(T^{k+1}_{i,j+1}-T^{k+1}_{i,j-1}+T^{k}_{i,j+1}-T^{k}_{i,j-1})$$
$$=\frac{T^{k+1}_{i,j-1}-2T^{k+1}_{i,j}+T^{k+1}_{i,j+1}+T^{k}_{i,j-1}-2T^{k}_{i,j}+T^{k}_{i,j+1}}{2Pr(\Delta R)^{2}}$$
$$+\frac{T^{k+1}_{i,j+1}-T^{k+1}_{i,j-1}+T^{k}_{i,j+1}-T^{k}_{i,j-1}}{4Pr[1+(j-1)\Delta R]\Delta R} \quad (13)$$

where $A=\dfrac{1}{1+\lambda 0.5(T^{k+1}_{i,j}+T^{k}_{i,j})}$

The region of integration is considered as a rectangle composed of the lines indicating X_{min}=0, X_{max}=1, R_{min}=1 and R_{max}=16 where R_{max} corresponds to R=∞ which lies very far from the momentum and energy boundary layers. In the above Eqs. (11)-(13) the subscripts i and j designate the grid points along the X and R coordinates, respectively, where X=i ΔX and R=1+(j−1) ΔR and the superscript k designates a value of the time t (=k Δt), with ΔX, ΔR and Δt the mesh size in the X, R and t axes, respectively. In order to obtain an economical and reliable grid system for the computations, a grid independence test has been performed. The steady-state velocity and temperature values obtained with the grid system of 100×500 differ in the second decimal place from those with the grid system of 50×250, and in the fifth decimal place from those with the grid system of 200×1,000. Hence, the grid system of 100×500 has been selected for all subsequent analyses, with ΔX=0.01, ΔR=0.03. Also, the time step size dependency has been carried out, which yields Δt=0.01 for a reliable result.

From the initial conditions given in Eq. (10), the values of velocity U, V and temperature T are known at time t=0, then the values of T, U and V at the next time step can be calculated. Generally, when the above variables are known at t=k Δt, the variables at t=(k+1) Δt are calculated as follows. The finite difference Eqs. (12) and (13) at every internal nodal point on a particular *i*-level constitute a tri-diagonal system of equations. Such a system of equations is solved by the Thomas algorithm [14]. At first, the temperature T is calculated from Eq. (13) at every j nodal point on a particular *i*-level at the (k+1)th time step. By making use of these known values of T, the velocity U at the (k+1)th time step is calculated from Eq. (12) in a similar manner. Thus the values of T and U are known at a particular *i*-level. Then the velocity V is calculated from Eq. (11) explicitly. This process is repeated for the consecutive *i*-levels; thus the values of T, U and V are known at all grid points in the rectangular region at the (k+1)th time step. This iterative procedure is repeated for many time steps until the steady-state solution is reached. The steady-state solution is assumed to have been reached when the absolute difference between the values of velocity as well as temperature at two consecutive time steps is less than 10^{-5} at all grid points.

The truncation error in the employed finite-difference approximation is $O(\Delta t^2+\Delta R^2+\Delta X)$ and tends to zero as ΔX, ΔR and Δt→0. Hence the system is compatible. Also, this finite-difference scheme is unconditionally stable as explained by Ganesan and Rani [15]. Stability and compatibility ensures convergence. The computations for the current problem have been carried out on an Intel Pentium 4 CPU 3.20 GHz computer system for different values of λ and Pr.

RESULTS AND DISCUSSION

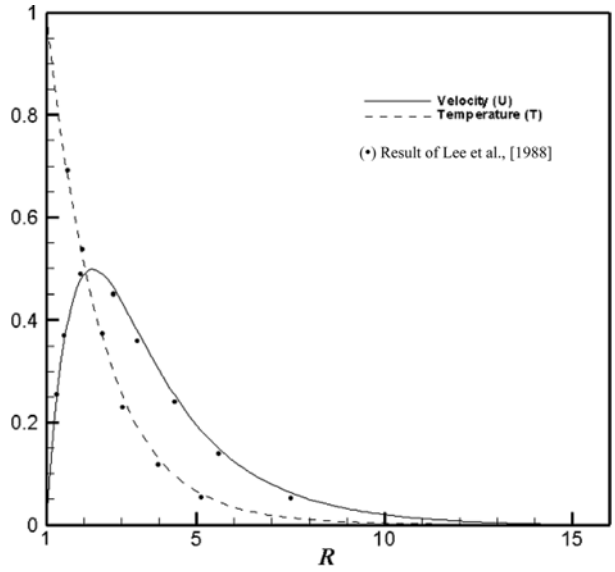

Fig. 2. Comparison of the velocity and temperature profiles for Pr =0.7 and λ=0.0.

To validate the current numerical procedure, the present simulated velocity and temperature profiles are compared with those of the available steady-state, isothermal and constant viscosity results of Lee et al. [4] for Pr=0.7, as no experimental or analytical studies exist for the present problem. The comparison results, which are shown in Fig. 2, are found to be in good agreement.

The simulated results are presented to outline the general physics involved in the effects of varying λ, the parameter measuring the strength of temperature dependence of the viscosity, and Pr on the transient velocity and temperature profiles. The computations are carried out for different values of the viscosity-variation parameter λ (=0, 1, 2, 3 and 4) and Pr (=7, 10, 20 and 30). The simulated transient behavior of the dimensionless velocity, temperature, aver-

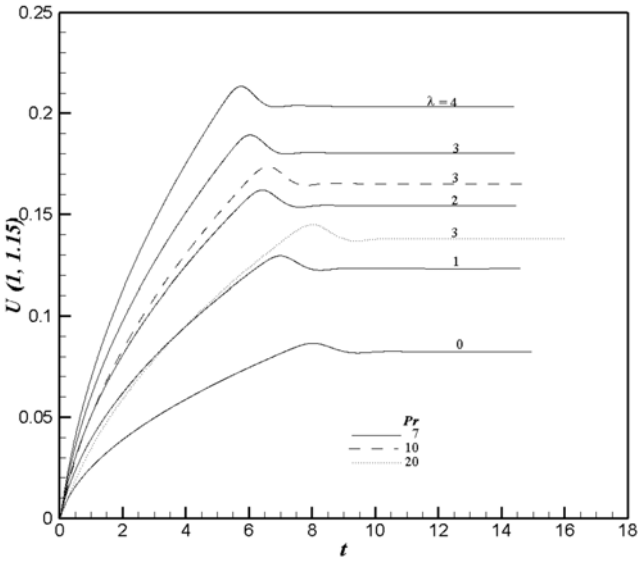

Fig. 3. The simulated transient velocity at (1, 1.15) for various λ and Pr.

age skin-friction and heat transfer coefficients is discussed in detail in the succeeding subsections.

1. Velocity

The simulated transient dimensionless velocity (U) at the location (1, 1.15) for various Pr and λ are graphically shown in Fig. 3 against the time (t). It is observed that the velocity increases with time, reaches a temporal maximum, then decreases and at last reaches the asymptotic steady-state. For example, when λ=4 and Pr=7, the velocity increases with time monotonically from zero and reaches the temporal maximum (U=0.218) at t=6, then slightly decreases with time and becomes asymptotically steady (U=0.205). The velocity at the other locations also exhibits similar transient behaviors and it is not presented here. This type of phenomenon was observed by several investigators for the problem of transient free convection on vertical cylinders and plates (Ekambavanan and Ganesan [16], Ganesan and Rani [15] and Rani [7]). At the very early time (i.e., $t \ll 1$), the heat transfer is dominated by conduction. Shortly later, there exists a period when the heat transfer rate is influenced by the effect of convection with the increasing upward velocities with time. And at the time when this transient period is almost ending and just before the steady state is about to be reached, there exist overshoots of the velocities. As denoted in Fig. 3, the magnitude of this overshoot of the velocities increases as λ is increased, since with the increasing λ the size of the term of velocity diffusion is decreased (refer to Eq. (8)), which yields less resistance to the fluid flow in the region of the temporal maximum velocities. In association with the transient characteristics of the velocity, similar trends of the temperature fluctuation can be observed as will be described in Fig. 6. The time needed to reach the temporal maximum of the velocity and the steady-state decreases with the increasing viscosity-variation parameter and decreasing Prandtl number. Thus, it can be concluded that the transient velocity profiles for fluids with variable viscosity differ from those with constant viscosity.

Figs. 4 and 5 show the simulated transient velocity profiles at the temporal maximum and steady-state against the radial coordinate R at X=1.0 for different λ and Pr, respectively. It is observed from these two figures that the velocity profiles start with the value zero at the wall, reach their maximum very close to the hot wall and then monotonically decrease to zero for all time t. From Figs. 4 and 5 it is observed that near the wall the magnitude of the axial velocity is rapidly increasing as the radial co-ordinate increases from R_{min} (=1).

In Fig. 4 the time to reach the temporal maximum of velocity and the steady-state clearly decreases with the increasing viscosity-variation parameter. But, the increasing values of the viscosity-variation parameter increase the velocity of the flow near the wall, because the viscosity is decreasing with the increase of the viscosity-variation parameter. The velocity reaches its maximum very close to the cylinder wall for higher values of λ. This qualitative effect

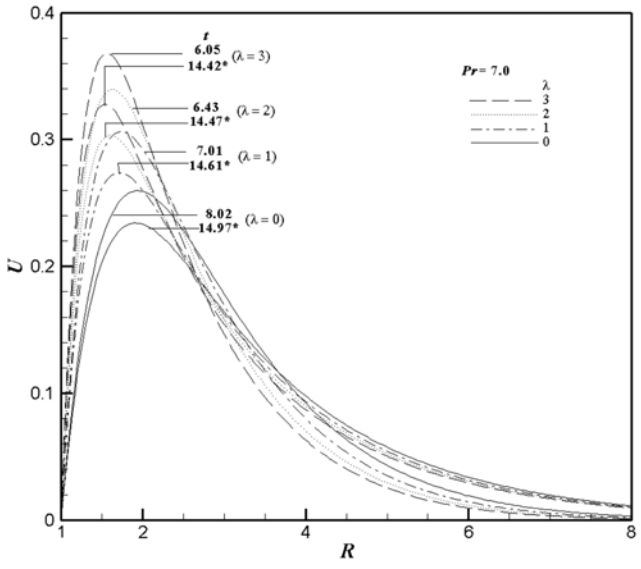

Fig. 4. The simulated velocity profiles at X=1.0 for Pr=7.0 and different λ (*-- Steady-state).

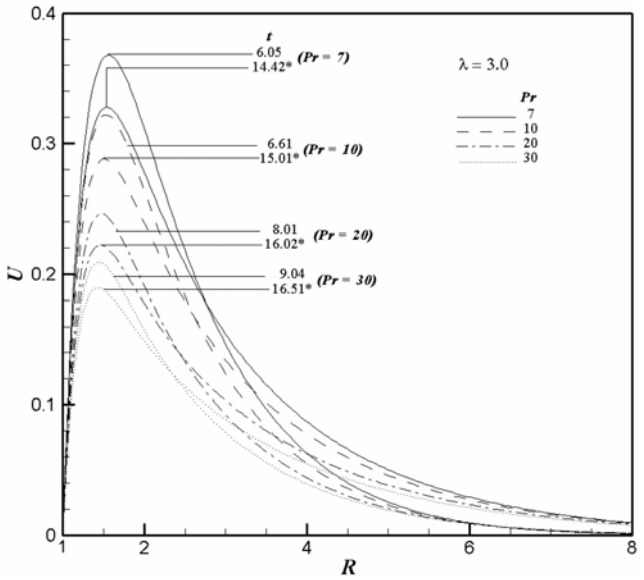

Fig. 5. The simulated velocity profiles at X=1.0 for λ=3.0 and different Pr (*-- Steady-state).

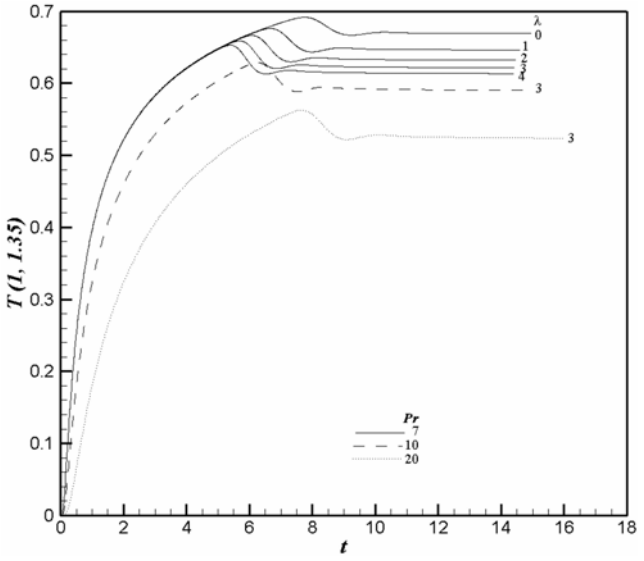

Fig. 6. The simulated transient temperature at (1, 1.35) for different λ and Pr.

arises because for the case of variable viscosity (λ>0) the fluid is able to move more easily in a region close to the heated surface in association with the fact that the viscosity of the fluid with λ>0 is smaller relative to the fluid with constant viscosity case. This results in thinner velocity and thermal boundary layers and hence increased surface heat transfer coefficients.

In Fig. 5 the time to reach the temporal maximum of the velocity and the steady-state increases with increasing Pr. Here, it is observed that the velocity decreases with the increasing Pr because the effect of velocity diffusion gets increased for high Pr. When Pr is increased, the thermal convection is confined to a region near the hot wall, while the momentum diffusion is propagated far from the hot wall and hence the high velocity profiles are observed to be close to the hot wall.

2. Temperature

The simulated transient temperature with respect to different Pr and λ values is shown at the point (1, 1.35) against the time in Fig. 6. Here, it is observed that the transient temperature profiles increase with time, reach a temporal maximum, decrease and again after slightly increasing attain the steady-state asymptotically. The temperature at other locations also exhibits somewhat similar transient behavior. During the initial period, the nature of the transient temperature profiles with respect to λ is particularly noticeable. The transient temperature profiles of fluids with variable viscosity (i.e., λ>0), initially coincide with and then deviate from the profiles of fluids with constant viscosity (i.e., λ=0). For example, when Pr=7 the temperature profile of λ=1.0 deviates from the temperature profile of fluid with constant properties (i.e., λ=0), say, for t≤7.0. Similarly, the temperature profile of λ=2.0 deviates from the temperature profile of λ=0 around t≥6.0. As seen before, during the initial time, the fluid with variable viscosity (λ>0) follows the characteristics of fluid with constant viscosity (λ=0) for each Pr. The concurrence period of the temperature profiles between λ>0 and λ=0, in the beginning, decreases with the increasing λ. It is also observed that the maximum temperature value decreases with the increasing

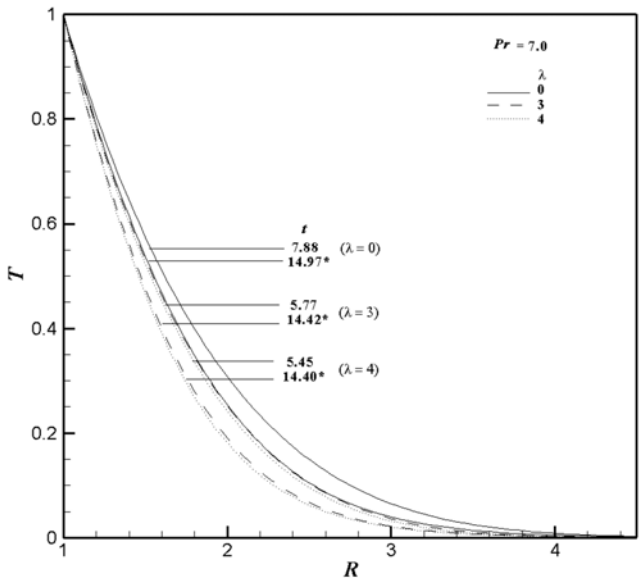

Fig. 7. The simulated temperature profiles for Pr=7.0 and different λ at X=1.0 (*-- Steady-state).

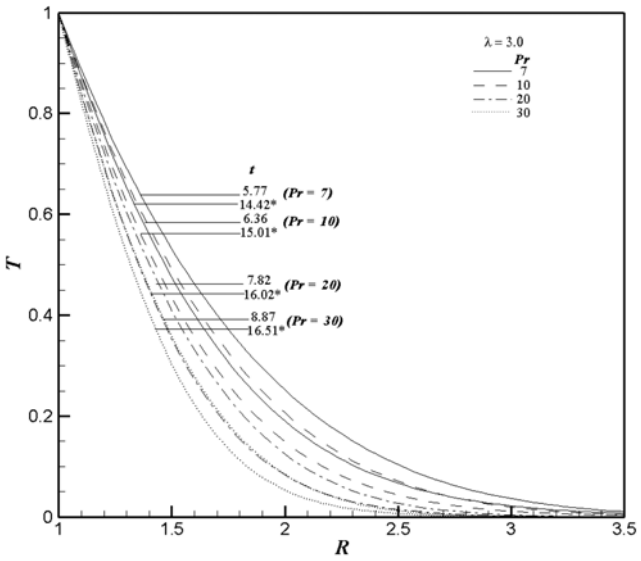

Fig. 8. The simulated temperature profiles for λ=3.0 and different Pr at X=1.0 (*-- Steady-state).

λ or Prandtl number.

The simulated transient temperature profiles at X=1.0 against the radial co-ordinate are shown in Figs. 7 and 8 for different λ and Pr, respectively. The temperature profiles start with the hot wall temperature (T=1) and then monotonically decrease to zero along the radial coordinate for all time t. Thinner temperature profiles are observed with the higher values of the viscosity-variation parameter. It is related to the fact that with the increase in the viscosity-variation parameter the viscosity of the fluid is decreasing, which allows for higher velocity near the hot wall. Also, the time to reach the temporal maximum of the temperature decreases with increasing λ and decreasing Pr. Larger Pr values give rise to thinner temperature boundary layer thickness, since a larger Pr value means that the thermal diffusion from the wall is not prevailing while the velocity diffusion tries to reach far from the wall.

3. Average Skin-friction Coefficient and Heat Transfer Rate

Having known the unsteady behavior of velocity and temperature profiles, it is interesting to study the average skin-friction coefficient and the average heat transfer rate (Nusselt number) and they are given by,

$$\overline{C_f} = \frac{Gr^{-2} r_0}{\mu_\infty \nu_\infty} \int \tau_w dx \tag{14}$$

$$\overline{Nu} = \frac{r_0}{k(T_w' - T_\infty')} \int q_w dx, \tag{15}$$

where $\tau_w = \left(\mu \frac{\partial u}{\partial r}\right)_{r=r_0}$ and $q_w = -k\left(\frac{\partial T'}{\partial r}\right)_{r=r_0}$

After the non-dimensional quantities (6) are introduced in Eqs. (14) and (15) they are reduced to the following form:

$$\overline{C_f} = \frac{1}{(1+\lambda)} \int_0^1 \left(\frac{\partial U}{\partial R}\right)_{R=1} dX \tag{16}$$

$$Nu = -\int_0^1 \left(\frac{\partial T}{\partial R}\right)_{R=1} dX \tag{17}$$

The derivatives involved in Eqs. (16) and (17) are evaluated by using a five-point approximation formula and then the integrals are evaluated by using the Newton-Cotes closed integration formula. The friction coefficient is an important parameter in the heat transfer studies since it is directly related to the heat transfer coefficient. The increased skin friction is generally a disadvantage in technical applications, while the increased heat transfer can be exploited in some applications such as heat exchangers, but should be avoided in others such as gas turbine applications, for instance. The simulated average non-dimensional skin friction and heat transfer coefficients have been plotted against the time in Figs. 9-12 for different λ and Pr.

The effects of viscosity-variation parameter λ and Prandtl number Pr on the simulated average skin friction coefficient are shown in Figs. 9 and 10, respectively. From Figs. 9 and 10 it is observed that for all values of λ and Pr the average skin friction coefficient increases with time, attains the maximum value and, after slightly decreasing, becomes asymptotically steady. It is also observed from Fig. 9 that for increasing values of λ the average skin-friction decreases. This result lies in the same line with the velocity profiles plotted in Figs. 4 and 5. Fig. 10 reveals that the increase in the value of Pr leads to a decrease in the values of the average skin friction coefficient.

In Figs. 11 and 12 the effects of viscosity-variation parameter λ and Prandtl number Pr on the simulated average heat transfer rate are shown, respectively. From Fig. 11, it is observed that for Pr=7,

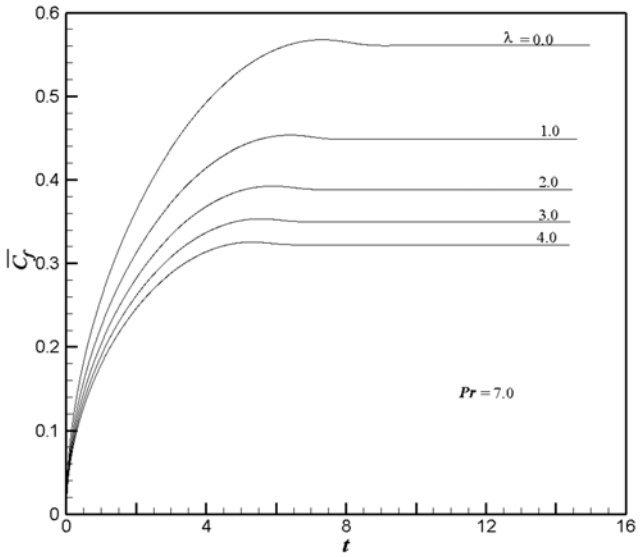

Fig. 9. The simulated average skin friction for Pr=7.0 and different λ.

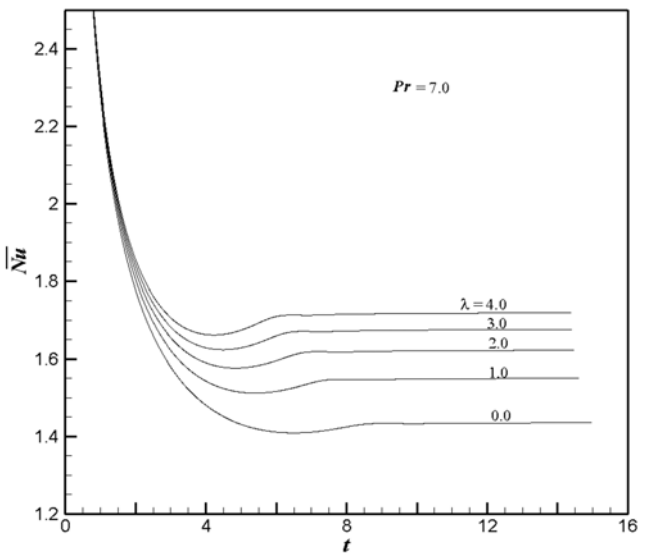

Fig. 11. The simulated average Nusselt number for Pr=7.0 and different λ.

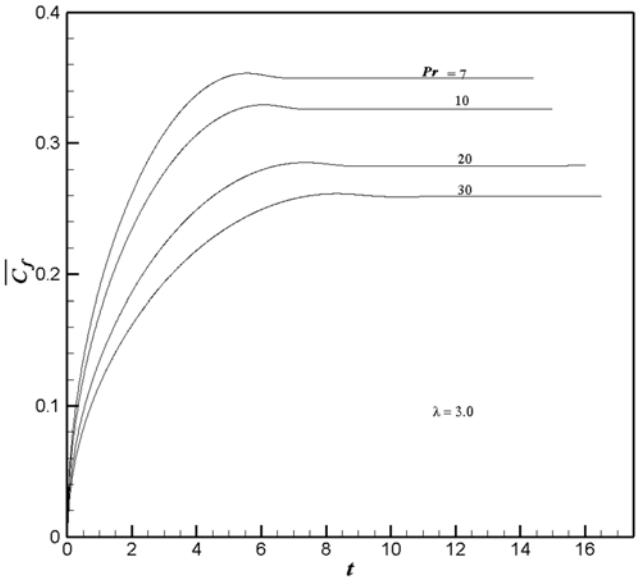

Fig. 10. The simulated average skin friction for λ=3.0 and different Pr.

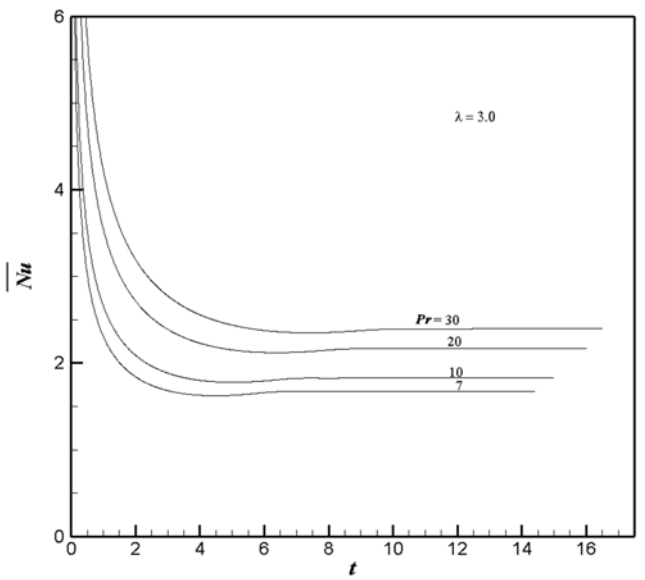

Fig. 12. The simulated average Nusselt number for λ=3.0 and different Pr.

the average heat transfer values for fluids with variable viscosity initially coincides with the case for the fluid with constant properties i.e., λ=0. Then it deviates from this smooth curve for λ=0 and reaches a steady-state asymptotically. This transient behavior of average heat transfer is in the same line with the transient temperature profiles with different λ shown in Fig. 6. From Fig. 11 it is seen that the average heat transfer rate increases monotonically with the increase of the viscosity-variation parameter λ. Fig. 12 reveals that an increase in the value of Pr leads to a increase in the values of the average heat transfer rate. Increasing Pr speeds up the spatial decay of the temperature field near the heated surface, yielding an increase in the rate of heat transfer.

CONCLUSIONS

A numerical study has been carried out for the unsteady natural convection along a semi-infinite vertical cylinder. A Crank-Nicolson type of implicit method is used to solve the dimensionless governing equations in a meridian plane. It has been assumed that the viscosity of the fluid is assumed to be temperature dependent. The computations are carried out for different values of the viscosity-variation parameter, λ (=0, 1, 2, 3 and 4) and Prandtl number, Pr (=7, 10, 20 and 30). For the velocity and temperature profiles it is observed that the time elapsed to reach the temporal maximum of the velocity and temperature and the steady-state decreases with the increasing λ and with the decreasing Pr. For each Pr, initially, the unsteady behavior of the flow characteristics such as the temperature and the average heat transfer rate for the fluid with variable viscosity (λ>0) coincides with that of the fluid with constant properties (λ=0). Then these flow characteristics of fluids with variable viscosity (λ>0) deviate from the fluid with constant properties (λ=0) and they reach the steady-state asymptotically. When the viscosity-variation parameter is larger, a higher velocity is observed in a region near to the wall, which gives higher average Nusselt number. The increase in the viscosity-variation parameter leads to an increase in the average heat transfer rate and a decrease in the average skin friction.

From the present study, it is observed that the results pertaining to the variable viscosity differ significantly from those of constant viscosity. The viscosity and Prandtl number of a working fluid have turned out to be sensitive to the variation of temperature in a natural convection problem. Hence, the effect of variable viscosity and Prandtl number has to be taken into consideration in order to predict the skin friction factor and heat transfer rate accurately.

REFERENCES

1. E. M. Sparrow and J. L. Gregg, *Trans. ASME*, **78**, 1823 (1956).
2. W. J. Minkowycz and E. M. Sparrow, *J. Heat Trans.*, **96**, 178 (1974).
3. T. Fujii and H. Uehera, *Int. J. Heat Mass Tran.*, **13**, 607 (1970).
4. H. R. Lee, T. S. Chen and B. F. Armaly, *J. Heat Tran.*, **110**, 103 (1988).
5. R. P. Dring and B. Gebhart, *Tran. ASME J. Heat Tran.*, **88**, 246 (1966).
6. K. Velusamy and V. K. Garg, *Int. J. Heat Mass Tran.*, **35**, 1293 (1992).
7. H. P. Rani, *Heat and Mass Tran.*, **40**, 67 (2003).
8. H. Schlichting, *Boundary layer theory*, McGraw-Hill, New York (1979).
9. J. Gray, D. R. Kassory and H. Tadjeran, *J. Fluid Mech.*, **117**, 233 (1982).
10. N. G Kafoussius and D. A. S. Rees, *Acta Mechanica*, **127**, 39 (1998).
11. M. A. Hossain, M. S. Munir and I. Pop, *Int. J. Thermal Sci.*, **40**, 366 (2001).
12. J. X. Ling and A. Dybbs, *J. Heat Tran.*, **114**, 1063 (1992).
13. M. M. Molla, M. A. Hossain and R. S. R. Gorla, *Heat Mass Trans.*, **41**, 594 (2005).
14. B. Carnahan, H. A. Luther and J. O. Wilkes, *Applied numerical methods*, John Wiley & Sons, New York (1969).
15. P. Ganesan and H. P. Rani, *Heat Mass Tran*., **33**, 449 (1998).
16. K. Ekambavanan and P. Ganesan, *Heat Mass Tran*., **30**, 63 (1994).